Noninvasive detection of spatiotemporal activation-repolarization interactions that prime idiopathic ventricular fibrillation

CARDIOLOGY

Noninvasive detection of spatiotemporal activation-repolarization interactions that prime idiopathic ventricular fibrillation

Matthijs J. M. Cluitmans[1,2]*, Laura R. Bear[3], Uyên C. Nguyên[1], Bianca van Rees[1], Job Stoks[1], Rachel M. A. ter Bekke[1], Casper Mihl[1,4], Jordi Heijman[1], Kevin D. Lau[2], Edward Vigmond[3], Jason Bayer[3], Charly N. W. Belterman[5], Emma Abell[3], Louis Labrousse[3,6,7], Julien Rogier[3,6,7], Olivier Bernus[3,6], Michel Haïssaguerre[3,6,7], Rutger J. Hassink[8], Rémi Dubois[3], Ruben Coronel[3,5], Paul G. A. Volders[1]

A comprehensive understanding of the interaction between triggers and electrical substrates leading to ventricular fibrillation (VF) and sudden cardiac arrest is lacking, and electrical substrates are difficult to detect and localize with current clinical tools. Here, we created repolarization time (RT) dispersion by regional drug infusion in perfused explanted human ($n = 1$) and porcine ($n = 6$) hearts and in a computational model of the human ventricle. Arrhythmia induction was tested with a single ventricular extrastimulus applied at the early or late RT region. Arrhythmias could only be induced from early RT regions. Vulnerability to VF increased with RT gradient steepness and with larger areas of early RT, but not with markers on the body-surface electrocardiogram. Noninvasive electrocardiographic imaging was performed in survivors of idiopathic VF ($n = 11$), patients with frequent premature ventricular complexes (PVCs) but no history of sudden cardiac arrest ($n = 7$), and controls ($n = 10$). In survivors of idiopathic VF, RT gradients were steeper than in controls, without differences in the clinical electrocardiogram, consistent with the ex vivo results. Patients with idiopathic VF also showed local myocardial regions with distinctly early-versus-late RT that were more balanced in size than in controls. Premature beats originated more often from the early RT regions in idiopathic VF survivors than in patients with frequent PVCs only. Thus, idiopathic VF emerges from the spatiotemporal interaction of a premature beat from an early-repolarization region with critical repolarization dispersion in that region. Electrocardiographic imaging can uncover the co-occurrence of these abnormalities.

INTRODUCTION

One in four cardiovascular deaths worldwide occurs suddenly and is often caused by ventricular fibrillation (VF) (*1*, *2*). Although sudden cardiac arrest (SCA) is often associated with ischemia or structural heart disease after infarction, these are absent in up to half of deaths (*1*, *3*). If no cause is identified, VF is diagnosed as "idiopathic" (*1*, *4*). Because nonstructural, purely electrical substrates are difficult to detect and localize with current clinical tools (*4*), a comprehensive understanding of the interaction between triggers and (subtle) electrical substrates leading to life-threatening arrhythmias in the structurally normal heart is lacking.

Electrical activation excites myocardial tissue and is followed by electrical recovery from inexcitability (repolarization). Abnormalities in repolarization can become arrhythmogenic even in the absence of structural abnormalities (*5*, *6*) and can lead to an abnormally early or late repolarization time (RT) of cardiac tissue. Regional differences in RT yield local RT gradients (RTGs), may promote reentry through unidirectional block of a next activation, and can form the basis for ventricular tachycardia (VT) and VF. The arrhythmogenic importance of RTGs has been shown previously in animal experiments (*6*) and patients (*7*, *8*). However, it is currently unknown how the steepness of RTGs and the relative sizes of the regions with disparate repolarization contribute to arrhythmia in relation to the coupling interval and spatial origin of the premature beat.

In addition, only overt repolarization abnormalities can be detected in current clinical practice, such as in the short- and long-QT syndromes. Subtle, regional repolarization abnormalities are likely not reflected in the clinical 12-lead electrocardiogram (ECG) (*1*). Recently, it has become possible to detect regional repolarization differences noninvasively in patients using electrocardiographic imaging (ECGI). (*7*–*12*) ECGI is a noninvasive technique to reconstruct electrical activity directly at the heart surface using approximately 200 electrodes at the torso surface and a geometrical representation of the heart and torso. It may provide more detailed and localized information than the ECG.

We hypothesized that the following elements are required for reentry to occur in the presence of a repolarization substrate: (i) myocardial regions of relatively early and relatively late repolarization, with a critically steep RTG in between; (ii) a critical size of the two regions; (iii) premature ventricular activation originating from a region that repolarizes relatively early; and (iv) critical timing of the premature ventricular activation. These abnormalities currently go largely undetected in patients because of insufficient accuracy of available clinical diagnostic modalities. To address these hypotheses, we combined electrophysiological studies on perfused explanted

[1]Cardiovascular Research Institute Maastricht, Maastricht University, 6200 MD Maastricht, Netherlands. [2]Philips Research, 5656 AE Eindhoven, Netherlands. [3]IHU LIRYC, 33600 Pessac, France. [4]Department of Radiology, Maastricht University Medical Centre, 6200 MD Maastricht, Netherlands. [5]Department of Experimental Cardiology, Amsterdam University Medical Centre, 1105 AZ Amsterdam, Netherlands. [6]University of Bordeaux, 33000 Bordeaux, France. [7]Hôpital Haut Lévêque, University Hospital of Bordeaux, 33604 Bordeaux, France. [8]Department of Cardiology, University Medical Centre Utrecht, 3584 CX Utrecht, Netherlands.
*Corresponding author. Email: m.cluitmans@maastrichtuniversity.nl

human and pig hearts with in silico modeling and applied the newly acquired insights to patients who survived VF undergoing noninvasive ECGI.

RESULTS

Figure 1 shows observations in a survivor of idiopathic VF. Figure 1A demonstrates the induction of polymorphic VT (later degenerating into VF) after a short-coupled premature beat (R-on-T phenomenon) as recorded by the standard 12-lead ECG. Clinical workup did not reveal a cause for the arrhythmia, but noninvasive ECGI allowed us to reconstruct local RT isochrones that highlighted a region with a short repolarization duration and steep RT dispersion (Fig. 1B). Figure S1 illustrates how the combination of such repolarization substrate and a trigger may lead to reentry.

Trigger-substrate interaction ex vivo shows increased arrhythmia susceptibility

We mimicked these clinical findings in an explanted heart setup with a perfused pig heart placed within a torso tank (Fig. 2A and fig. S2). Local arrhythmia inducibility was tested at baseline, during local drug infusion (drug concentrations are specified in table S1), and after drug washout. During drug infusion, the posterior side (POST) of the heart was first infused with the repolarization-prolonging drug dofetilide, and later, the anterior side of the heart was simultaneously infused with the repolarization-shortening drug pinacidil [through the left anterior descending (LAD) artery]. Local unipolar electrograms (EGMs) were recorded directly at the heart surface to determine the local RT. The epicardial RT isochrones during a typical experiment showed that drug infusion resulted in two distinct regions with pronounced early and late RT and a transition with steep RTGs (Fig. 2B) that normalized after drug washout. At the heart surface, the repolarization waves in the local unipolar EGMs changed from positive (early RT region) to negative (late RT region) over the RTGs (Fig. 2C and fig. S3). We confirmed that the repolarization wave upslope of the epicardial EGM was a good marker of RT and of the time of recovery from inexcitability (fig. S4).

Arrhythmia induction was tested with an S1-S2 protocol by providing a single ventricular programmed stimulus (S2) after a train of eight atrial paced beats (S1). In a typical explanted pig heart (Fig. 3A), atrial pacing resulted in a homogeneous activation of the ventricles through the native conduction system. Repolarization was more heterogeneous because of local drug infusion, with distinct regions of early and late RT (Fig. 3B). The activation isochrones of a subsequent single ventricular S2 stimulus from the early RT region (Fig. 3C) showed that this premature beat blocked against the RTG, traveled around the gradient, and then reactivated the previously refractory tissue (unidirectional block). This resulted in a sustained arrhythmia (Fig. 3D) that was maintained by a reentry circuit along electrodes a to f with continuous reactivation of the tissue (Fig. 3E).

These observations were confirmed in a series of six pig heart experiments (Fig. 3, F to H). Although the heart rate corrected QT interval (QTc) determined from the body-surface ECG during maximum drug infusion did not differ from the baseline condition, the RTGs determined from the ventricular EGMs were increased ($P = 0.02$; Fig. 3F). In the presence of drug-induced RTGs, arrhythmia inducibility increased (Fig. 3G). Arrhythmias could only be induced when pacing from the early RT region (LAD) and not from the late RT region (POST; Fig. 3H). The QTc interval was not different between inducible and noninducible hearts (fig. S5A). Conversely, the maximum RTG was a significant arrhythmia predictor ($P < 0.05$; fig. S5B). Also, in the explanted human heart, arrhythmias could only be induced from the early RT region and only in the presence of a steep (drug-induced) RTG (fig. S6).

Figure 3I shows examples of the S1-S2 induction protocol with the "R-on-T" phenomenon on lead II of the tank-surface ECG. Despite the presence of an R-on-T morphology, arrhythmia induction was absent if repolarization heterogeneity was absent or if the premature stimulus was applied to the late repolarizing region.

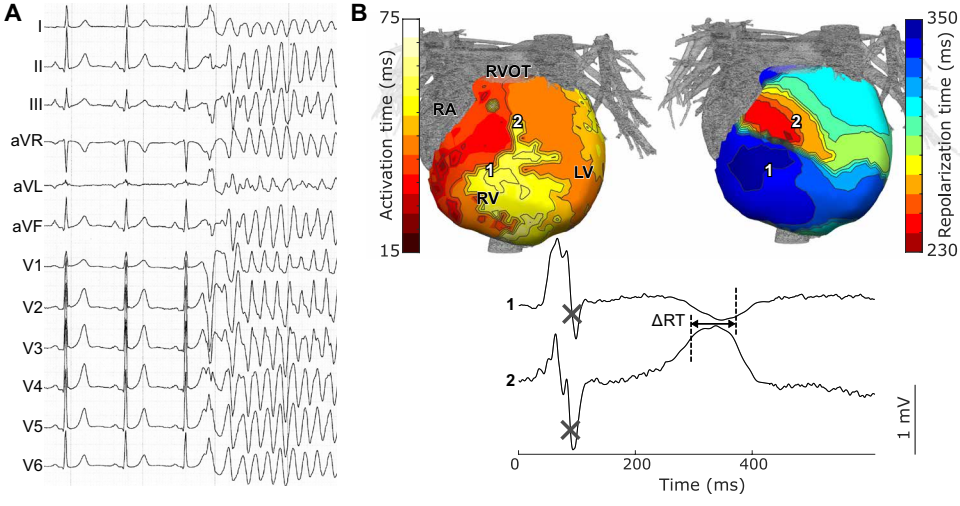

Fig. 1. Electrocardiographic findings in a patient who suffered from idiopathic ventricular fibrillation. The patient's 12-lead ECG (**A**) shows the initiation of a polymorphic ventricular tachycardia, induced by a single premature beat occurring closely to the preceding repolarization (R-on-T phenomenon). Noninvasively mapped activation time and repolarization time (RT) isochrones during sinus rhythm (**B**) demonstrate apparently normal electrical activation pattern but locally dispersed RTs. Unipolar electrograms (EGM) demonstrate a large local RT difference (arrow). X, activation time marker; RVOT, right ventricle outflow tract; RA, right atrium; RV, right ventricle; LV, left ventricle. Vertical dashed lines represent RT marker.

The spatiotemporal vulnerability to arrhythmias increases with stronger repolarization abnormalities

We next studied the spatial and temporal vulnerability to arrhythmias in the explanted hearts and in a computer model. The computational experiments were performed with a previously published human ventricular model (*13*) in which the local potassium channel conductance was changed to create a region of variable size with early RT and a region with late RT (Fig. 4A). Arrhythmia inducibility was tested with an S1-S2 protocol on multiple locations. In agreement with the ex vivo observations, the computer model showed that arrhythmias could only be induced with an S2 stimulation in early RT regions and not in late RT

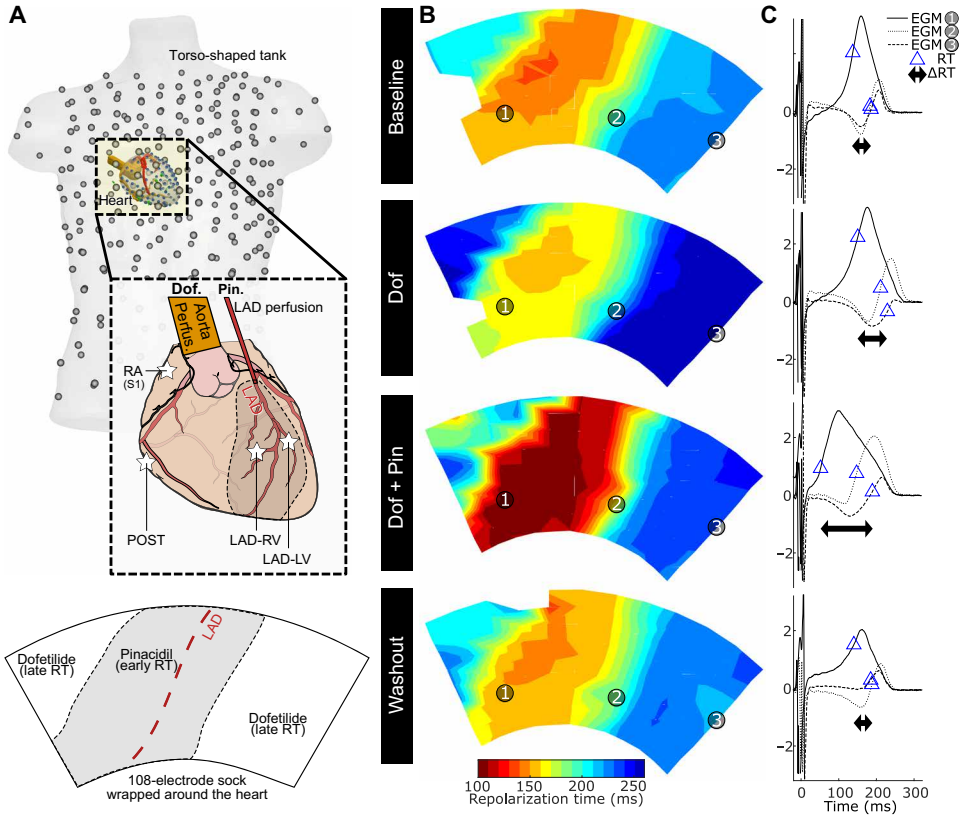

Fig. 2. Local drug infusion produces RT gradients reflected by local EGM changes. (**A**) Explanted hearts are placed in a torso-shaped tank; gray dots on the torso indicate torso-surface electrodes; blue dots on the heart indicate the heart-surface (sock) electrodes. The hearts have different perfusion beds of the left anterior descending (LAD) artery and the remaining (aorta-perfused) region. These regions are infused with pinacidil (Pin.) and dofetilide (Dof.), respectively, creating substantial RT gradients (RTGs) between the perfusion beds. Pacing electrodes (stars) are positioned at the right atrium, the LAD perfused regions (LAD-LV and LAD-RV), and the posterior, non-LAD perfused, region (POST). Unipolar epicardial EGMs were recorded with a 108-electrode sock. (**B**) Representative results from an explanted pig heart show RT isochrones at baseline (row 1), when locally infusing dofetilide (Dof; row 2), when infusing dofetilide and pinacidil (Dof + Pin; row 3), and during washout (row 4). (**C**) During baseline (S1) pacing, selected sock EGMs in the early (EGM 1) and late (EGM 3) RT region and the transition zone (EGM 2) show the resulting repolarization-wave morphology changes. The RT dispersion increases during drug infusion (black arrow). The moment of steepest EGM repolarization-wave upslope (reflecting local RT) is indicated by the blue triangle.

regions (Fig. 4B and figs. S7 to S9). These simulations also showed that the maximum temporal vulnerable window (the range of S1-S2 intervals resulting in arrhythmias) increased with the steepness of the RTG, but not with the size of the area of early RT (Fig. 4C). This was in agreement with the observations from the explanted heart experiments (Fig. 4D). Conversely, the simulations show that the size of the spatial vulnerable region (reflected by the number of arrhythmia-inducing pacing locations) increased mainly with the size of the area of early repolarization above a threshold RTG (Fig. 4E). In the explanted heart experiments, the size of the early RT region could not be changed, but the number of vulnerable locations did increase with steeper RTGs (Fig. 4F).

Observations in survivors of idiopathic VF uncover repolarization abnormalities

We then studied the clinical relevance of these findings. Patients were determined to have idiopathic VF if they had documented VF but no identifiable cause during extensive clinical workup (*4*). Patients were included in the premature ventricular complex (PVC) group if they had frequent monomorphic PVCs requiring catheter ablation but had no history of SCA, VT, or VF and no structural abnormalities on echocardiography or magnetic resonance imaging (MRI). Control subjects had no history of cardiac arrhythmias, a normal ECG, a normal computer tomography angiography, and no structural abnormalities. All patients underwent ECGI as previously described (see fig. S10) to reconstruct epicardial ventricular unipolar EGMs, activation times, RT, and RTGs for selected beats (*11*, *12*). Table 1 and table S2 show characteristics of the three groups of patients.

Representative examples from each group are shown in Fig. 5. In all three examples, ECGI identified regions of local RT differences, but they were most pronounced in patients with VF (Fig. 5A). In agreement with the explanted heart observations, local reconstructed EGMs at the heart surface (Fig. 5B) typically showed a repolarization wave that changed polarity between these regions of pronounced local RT differences. RT isochrones and histograms (Fig. 5C) showed relatively large regions of early RT in the patient with idiopathic VF; PVCs emerged from this region in the patient with idiopathic VF, but from the late RT region in the patient with PVCs. Regions with pronounced RT differences resulted in steep local RTGs (Fig. 5D).

Survivors of idiopathic VF have clinically concealed repolarization abnormalities

Standard clinical markers for repolarization (QTc and Tpeak-Tend intervals on the 12-lead ECG) were not significantly different between the patient groups (Fig. 6, A and B): $P = 0.29$ and 0.057 for QTc and $P = 0.91$ and 0.22 for Tpeak-Tend, for PVC versus control and idiopathic VF versus control, respectively. However, ECGI uncovered significantly more RT heterogeneity with steeper RTGs in survivors of idiopathic VF than in controls (Fig. 6D): $P = 0.47$ for PVC versus control and $P = 0.02$ for idiopathic VF versus control. This was also true for alternative metrics of local RT heterogeneity such as local RT dispersion (fig. S11). Histograms of the epicardial RTs (Fig. 5C) showed multiple peaks, corresponding to the presence of organized regions with early and late repolarization. Survivors of idiopathic VF typically had more peaks in the RT histogram (figs. S12 and S13). Their "surface ratio" (the ratio of surface areas of the two largest RT regions) was significantly closer to 1, indicating that those relatively early and late RT zones were similar in size, whereas in the other patient groups, one RT zone was much larger than all other zones (Fig. 6E): $P = 0.25$ for PVC versus control and $P = 0.005$ for idiopathic VF versus control.

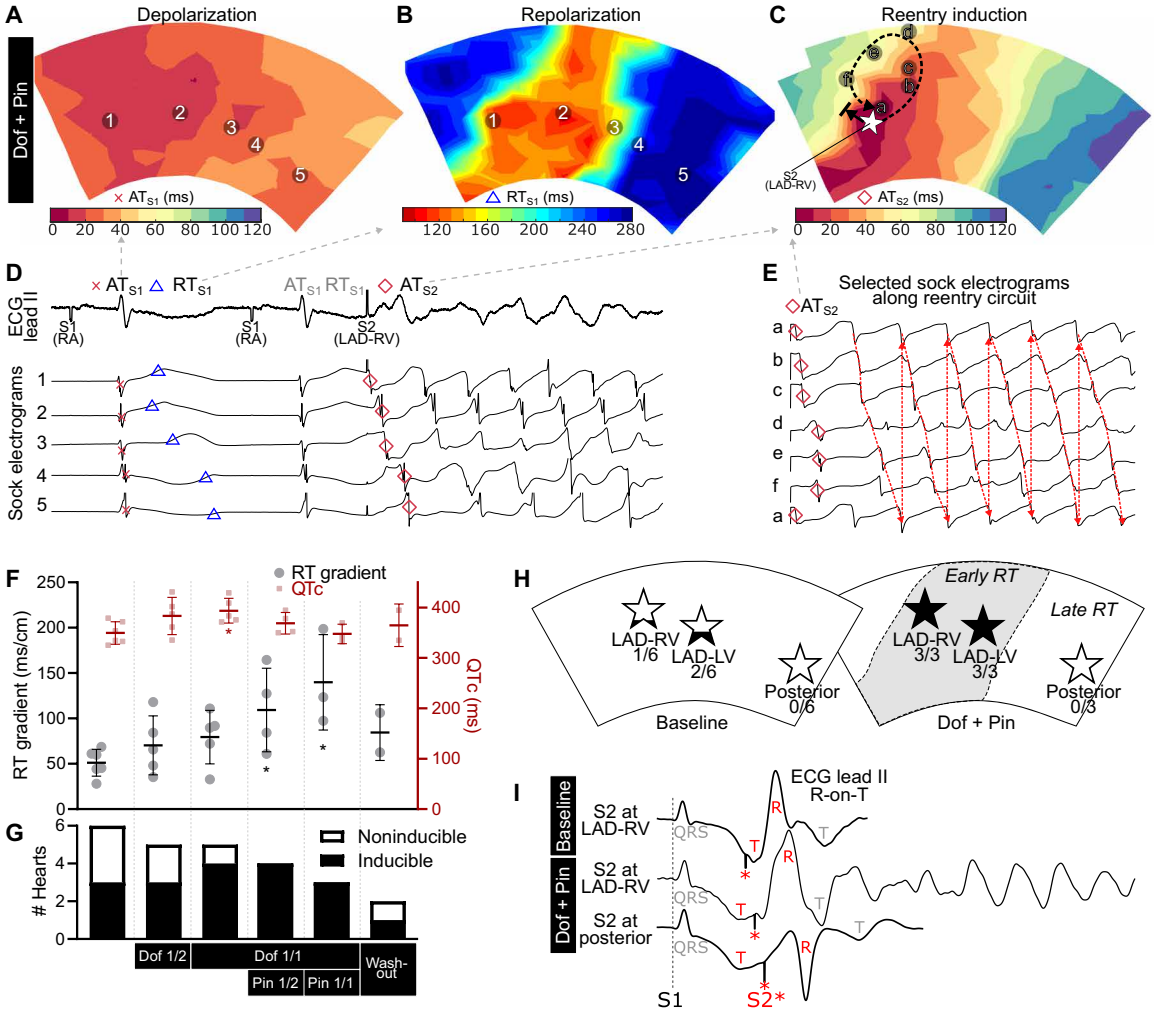

Fig. 3. Induction of ventricular fibrillation on a RT substrate in explanted pig hearts. (**A**) During maximum drug infusion, ventricular activation by atrial pacing (S1) is fast and homogeneous, but repolarization (**B**) is heterogeneous with clear RTGs flanking the early-repolarizing region. (**C**) A short-coupled ventricular stimulus (S2; star) from the early RT region activates the heart with unidirectional block against the RTG. (**D**) Local EGMs show dispersion of RT during S1 pacing with activation block at the RTGs (electrodes 3 and 4) after the S2 stimulus. (**E**) After the initial unidirectional block, the S2 activation wavefront continues to propagate along a reentry circuit near electrodes a to f. (**F**) Data from all six explanted pig hearts show that RTGs increase with drug infusion, but the body-surface QTc marker is largely unchanged, especially during maximum RTGs. (**G**) Drug infusion and larger RTGs correspond to higher inducibility of reentrant arrhythmias. (**H**) Arrhythmia induction occurs only when the S2 stimulus is from the early RT region. (**I**) EGM lead II shows an R-on-T phenomenon for any short-coupled S2 stimulus but yields reentry only when pacing from the early RT region in the presence of RTGs.

Survivors of idiopathic VF had relatively large regions of early RT (fig. S12).

Thus, ECGI showed that idiopathic VF survivors had regions of relatively early and late RT, with relatively large early RT regions, and steep RTGs. This was true even after excluding two idiopathic VF survivors who had a left-bundle-branch-block morphology on their clinical ECG (fig. S14).

Premature beats manifest from early-repolarizing regions in survivors of idiopathic VF

In most patients from the idiopathic VF group, PVCs occurred frequently (table S2). In line with literature findings (*14*), the shortest coupling interval for PVCs (the interval to the preceding beat) was shorter for patients in the idiopathic VF group than for patients in the PVC group (Fig. 6C): $P = 0.027$. Patients from the PVC group predominantly displayed extrasystoles manifesting from regions that showed late repolarization during sinus rhythm, whereas idiopathic VF survivors more often had PVCs manifesting from early-repolarizing regions (Fig. 6F): 7 of 11 idiopathic VF survivors versus 1 of 7 PVC individuals had their PVCs originate from the early RT region ($P = 0.04$). In three idiopathic VF survivors, ECGI captured a "clinically suspect" PVC (a PVC that on 12-lead ECG initiated a sustained or nonsustained VT). In two of three cases, ECGI identified the macroscopic origin of this PVC well within the early RT region (figs. S15 and S16); in the other case, it appeared to come from the late side of the RTG, but its distance to the gradient fell within the spatial uncertainty of ECGI. These observations are in agreement with our ex vivo and in silico results: The temporal

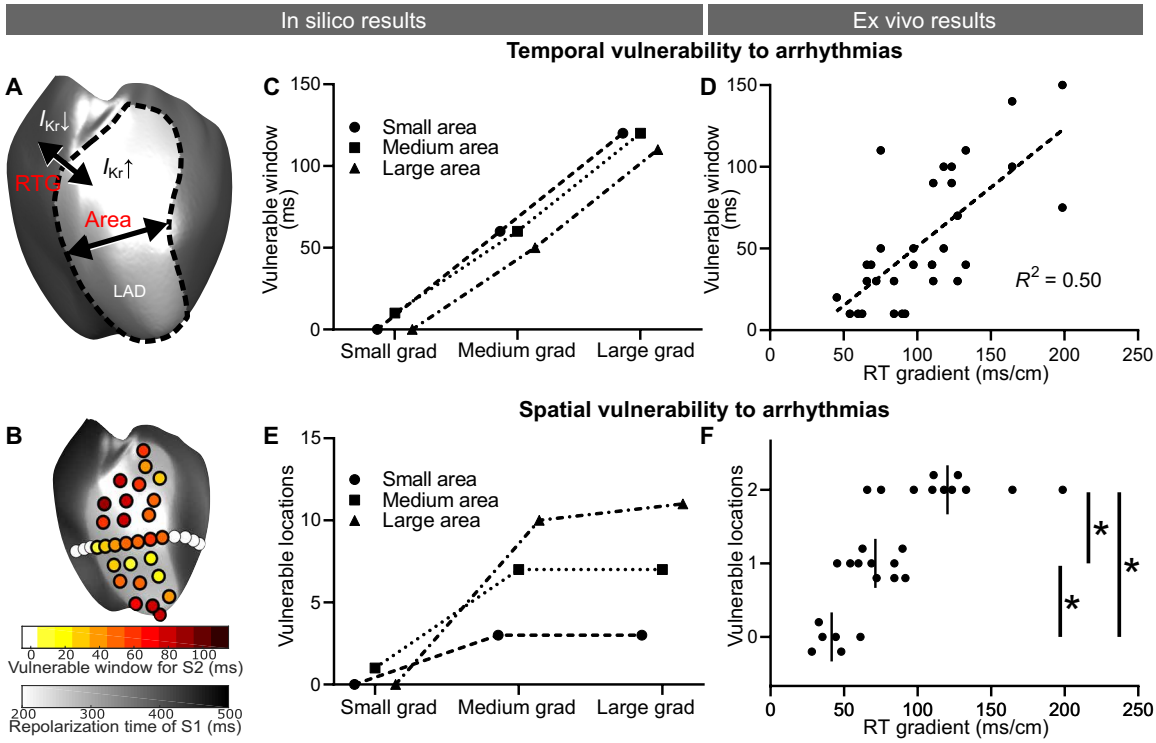

Fig. 4. Temporal and spatial vulnerability for arrhythmias increases with steeper RTGs and larger early-repolarization regions. (**A**) In a computational model of a human ventricle, different RTGs and different sizes of the area of early RT were created. (**B**) Arrhythmia inducibility was tested for various locations; the color reflects the size of the temporal vulnerable window (white indicates that no arrhythmia could be induced). This was tested for nine combinations of small, medium, or large gradients and small, medium, or large early RT areas. (**C**) The temporal vulnerable window increased with the steepness of the RTG but was independent of the size of the early RT area. (**D**) In the explanted hearts (with a fixed area of early RT), a similar dependency between vulnerable window and RTG was found. (**E**) The computational model demonstrated that the spatial vulnerable region increased with a larger size of the early RT area, although only for RTGs of sufficient size. (**F**) The explanted hearts showed an increasing number of inducible pacing locations at the early RT region with steeper RTGs. *$P < 0.05$.

Table 1. Presence of key trigger-substrate arrhythmia elements in humans.

	Control ($n = 10$)	PVC ($n = 7$)	Idiopathic VF ($n = 11$)	Difference from control
Patients with potential RT substrate*	1 (10%)	1 (14%)	7 (64%)	$P = 0.02$
Patients with potential trigger†	0 (0%)	1 (14%)	6 (55%)	$P = 0.01$
Patients with substrate and trigger‡	0 (0%)	0 (0%)	5 (45%)	$P = 0.02$

*Substrate defined as sinus rhythm RTGs > 200 ms/cm and RT surface ratio > 0.4. †Defined as a PVC from a region that has an early RT during sinus rhythm. ‡Defined as the simultaneous presence of the previously defined substrate and trigger.

(R-on-T) and the spatial relationship of a premature beat to the preceding repolarization pattern are key determinants of risk for arrhythmia induction.

Simultaneous occurrence of triggers and substrate is common in survivors of idiopathic VF

Next, we determined the presence of a repolarization substrate in each individual using the following cutoff values: (i) a maximum RTG of >200 ms/cm and (ii) an RT surface ratio of >0.4 (Table 1 and table S3). This substrate was present more often in survivors of idiopathic VF than in controls ($P = 0.02$). PVCs originating from the early RT region also occurred more often in survivors of idiopathic VF ($P = 0.02$). The combined observation of substrate (steep RTG with high RT surface ratio) and trigger (PVCs from early RT regions) was only present in survivors of idiopathic VF ($P = 0.02$). A Venn diagram illustrates the increased co-occurrence of these ECGI-identified abnormalities in the idiopathic VF group compared to the other groups (Fig. 6G).

Figure S20 (A to C) shows a patient case that illustrates our main clinical findings. It represents the heart of an idiopathic VF survivor with steep RTGs (fig. S20A) and frequent PVCs that have their macroscopic breakthrough at an early RT region (fig. S20B). A subtle

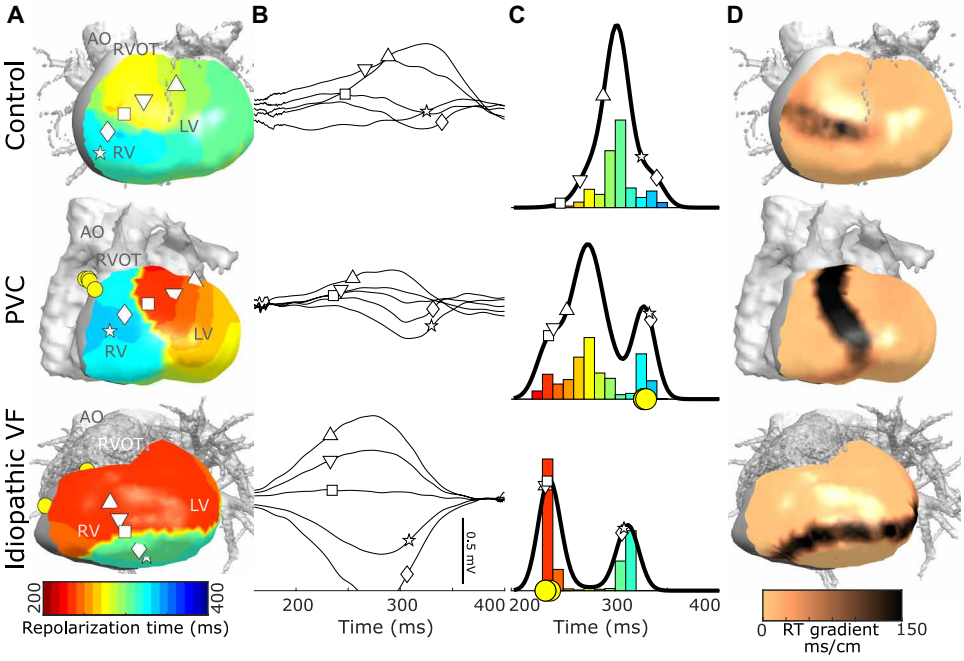

Fig. 5. Noninvasive mapping of repolarization substrate and premature beats in a control, a patient with frequent premature beats only, and a patient who survived idiopathic ventricular fibrillation. Electrocardiographic imaging (ECGI) was used to study repolarization characteristics for a typical control, and individuals with premature ventricular complex (PVC) and idiopathic ventricular fibrillation (iVF). (**A**) Ventricular RT isochrones highlight RTGs for a sinus beat. (**B**) Selected epicardial unipolar EGMs show the morphology changes across the RTG. Symbols in the EGMs correspond to their location in (A). The symbol position in (B) reflects the local RT (repolarization-wave upslope) in the EGM. (**C**) Histograms of all RTs during a sinus beat may show multiple distinct regions of RT. Yellow circles indicate the spatial origin of PVCs [in (A)] and the sinus beat RT corresponding to that region [in (C)]. (**D**) Local RTGs are shown. AO, aorta.

change in PVC origin or timing may fulfill all requirements of the arrhythmia hypothesis to explain the patient's SCA (fig. S20C).

DISCUSSION

Our combined data demonstrated that a critical interaction of four factors determines the inducibility of reentry in a setting of purely electrical substrate (fig. S20D): (i) the timing of the inducing premature beat, (ii) its macroscopic origin location from a region of early repolarization, (iii) the presence of a steep RTG, and (iv) the relative sizes of the tissue with long and short repolarization. The stronger the abnormalities, the larger the spatiotemporal arrhythmia vulnerability: Steeper RTGs result in a larger temporal vulnerability (Figs. 4, C and D, and 6D), whereas a larger region of early repolarization results in larger spatial vulnerability (Figs. 4E and 6E). Survivors of idiopathic VF have steeper RTGs and more spatially size-balanced regions of RT abnormalities compared to controls, and PVCs' origins manifest more often from an early RT region. These abnormalities were not evident on the standard 12-lead ECG but were unmasked by ECGI. Exercise or other provocative conditions may lead to further abnormalities being uncovered (*15*). Alternative metrics on the 12-lead ECG may contain more information than the QTc or Tpeak-Tend interval (*16*), because these intervals are a measure of repolarization duration and repolarization heterogeneity in the entire heart. The 184-lead ECG shows a broader T wave in survivors of idiopathic VF than in controls (fig. S13). ECGI may allow better identification of patients at risk for idiopathic VF, in particular when combining multiple ECGI metrics (Fig. 6G) in the absence of lethal arrhythmias; this may hold promise to identify such patients before their arrhythmia occurs.

There are several important limitations to our study. In the explanted heart experiments and computer models, the effect of electromechanical coupling, central nervous system, and other systemic effects could not be studied. These factors are strong modulators of repolarization heterogeneity (*17*) and have been detected by ECGI. Although the ex vivo and in silico studies focused on reentry initiation (and did not differentiate between subsequent VT or VF), our ECGI observations were performed in patients who had VF. In our ex vivo experiments, most induced arrhythmias appeared to be polymorphic VT or VF. Further investigations are required to study how reentry initiation subsequently develops to VF. Because of the relatively rare occurrence of idiopathic VF, only a limited number of patients could be included, and ECGI was performed in the absence of spontaneous arrhythmias.

We surmise that the spatiotemporal trigger-substrate interaction concept can be applied to other electrical diseases of the heart. For example, in long-QT syndrome (LQTS), repolarization is prolonged to such an extent that it is detectable from the clinical ECG, but not all patients with overt LQTS have a similar risk for SCA (*18*). Experimental results have confirmed our hypothesis that it is not the absolute (homogeneous) prolongation of RT, but the local differences in RT that determine arrhythmia susceptibility (*19*). The application of ECGI in clinical cohorts of patients with LQTS and Brugada syndrome has suggested that the presence and steepness of RTGs are associated with arrhythmia risk (*7*, *8*). In the early-repolarization syndrome, although its underlying mechanisms (abnormalities in depolarization or early phase 2 repolarization) may not directly link to an actual early end of (phase 3) repolarization, arrhythmogenic patients had steeper RTGs than controls (*9*). On a smaller scale, RTGs may exist between the voluminous and relatively slow-conducting myocardium and the fine and fast-conducting Purkinje network and may play a role in particular for Purkinje-mediated premature beats (*20*).

The concept of R-on-T is classically associated with arrhythmia risk, but, as we show here, it is not sufficient to explain VF initiation. Also, in the setting of ischemia, R-on-T PVCs may occur frequently without inducing arrhythmias (*21*). Conversely, SCA is frequently initiated in the absence of R-on-T (*22*), but it is currently unknown whether the premature beat may then be on top of clinically concealed repolarization abnormalities of sufficient magnitude. It has been suggested that steep RTGs may generate triggers (*23*). In our ex vivo experiments, we did not typically observe spontaneous

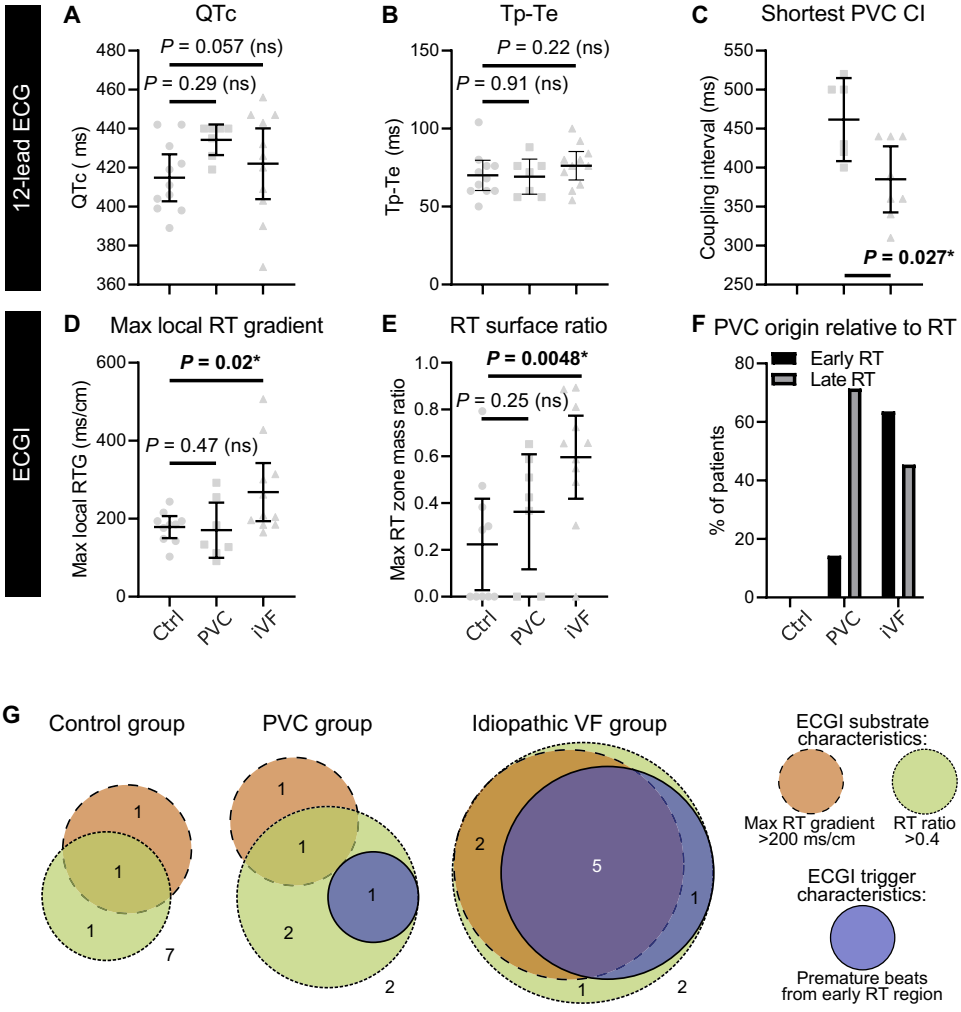

Fig. 6. Noninvasive mapping in patients with idiopathic ventricular fibrillation uncovers a repolarization substrate and its relation to premature beats. Group statistics for all individuals for the standard 12-lead ECG (A to C) and ECGI (D to F). Scatter plots display mean (horizontal line) and 95% confidence interval (whiskers). (**A**) Heart rate corrected QT intervals (QTc) and (**B**) Tpeak-Tend interval from the clinical 12-lead ECG on the standard ECG. (**C**) The shortest observed coupling interval (CI) of PVCs on standard ECG is earlier in idiopathic VF survivors. (**D**) ECGI reveals that the maximum local RTG and (**E**) the ratio between the "surface" (histogram count) of the two largest RT regions are larger in idiopathic VF survivors. (**F**) PVC origins categorized as coming from a region with early versus late RT during sinus rhythm. (**G**) A Venn diagram illustrates the occurrence of ECGI-identified substrate and trigger abnormalities, highlighting an increased concurrent occurrence in survivors of idiopathic VF. *$P < 0.05$; ns, not significant.

PVCs at baseline or in the presence of steep RTGs. Also, the origin of clinically suspect premature beats was not necessarily located at the RTG in survivors of idiopathic VF (fig. S15). However, we did not investigate modulating factors such as adrenergic stimulation, which have been suggested to generate spontaneous beats from regions of large RT heterogeneity ("R-from-T") (*23*). Convincing evidence also suggests a key role of Purkinje cells in generating triggering PVCs in idiopathic VF (*20*). This is within the scope of our findings, as in this study we could only observe the apparent (macroscopic) epicardial breakthrough of PVCs and not their (microscopic) cellular origin. The observed PVCs in the idiopathic VF group may very well be Purkinje-mediated, and further studies are required to confirm this. More research is also needed to explain the apparent breakthrough of PVCs at an early-repolarizing region, which could be either mechanistic (early triggers from Purkinje cells can only exit the Purkinje system at locations with excitable myocardium, thus early-repolarizing regions, or RTGs intrinsically generate triggers that then can only excite early-repolarizing regions) or stochastic (triggers from the Purkinje system may develop anywhere but will only induce VF when originating from an early-repolarizing region).

Here, we studied VF initiation based on a single ventricular beat on top of preceding sinus rhythm RT heterogeneity. This concept may be extended to arrhythmias that start with multiple focal beats by considering the interaction of a focal beat with the RT of the previous focal beat. In addition, RT is the summation of local activation time and local duration of repolarization, and in our ex vivo and in silico experiments, we studied heterogeneity in repolarization duration. RT heterogeneity may also result from heterogeneity in activation, for example, due to zigzag conduction through small conducting channels within the permanently inexcitable scar (*24*), sodium channel abnormalities (*25*), or post-repolarization refractoriness (*26*). Considering these various sources of "excitability heterogeneity" would allow us to extend our reasoning to other myocardial substrates or even arrhythmias of other electromechanical organs. For example, the role of (premature) activation and conduction block has been recently studied in dysrhythmias of the gastrointestinal system (*27*) and uterus (*28*), but the role of excitability dispersion in such organs is still unknown.

Our proposed concept has implications for diagnosis, risk stratification, and preventive therapy of idiopathic VF. Noninvasive methods such as ECGI now enable detection of the four identified conditions and suggest selective therapy targeted to one or more of the four spatiotemporal trigger-substrate elements (fig. S20D) to prevent SCA, although this will require further study. For example, if PVCs occur frequently in the presence of RT heterogeneities and from an early RT region, one may consider aggressive therapy to reduce the RTGs or abolish the PVCs. In particular, previous studies suggest that Purkinje-mediated PVCs play an important role in idiopathic VF (*20*) and indicate that PVC ablation prevents the recurrence of SCA (*29*).

In this study, we identified critically timed activation-repolarization interactions to prime arrhythmogenesis, in which spatial vulnerability increased with the size of early RT regions and temporal vulnerability with the steepness of RTGs. These findings provide a comprehensive and clinically relevant perspective on the trigger-substrate

interaction resulting in VF and suggest avenues for risk stratification of life-threatening arrhythmias.

MATERIALS AND METHODS

Study design

Here, we studied RT heterogeneity in explanted pig and human hearts, in computer models, and in humans. The goal was to study the presence of RT heterogeneity in survivors of idiopathic VF and to better understand the interaction between triggers and RT substrate in ex vivo and in silico hearts.

Patients were recruited at Maastricht University Medical Center with approval from the local ethical committee (ClinicalTrials.gov NCT03947021). Patients were included in the idiopathic VF group if they had documented VF but no identifiable cause during extensive clinical workup. Diagnostic procedures to exclude known causes of VF were based on (exercise) ECG, blood chemistry, toxicological screening, Holter monitoring, echocardiography, coronary angiography or computed tomography angiography (CTA), MRI, and targeted genetic testing (*4*). Patients were included in the PVC category if they had frequent monomorphic PVCs requiring catheter ablation but had no history of SCA, VT, or VF and no structural abnormalities on echocardiography or MRI. Control subjects had no history of cardiac arrhythmias, a normal ECG, and a normal CTA and no structural abnormalities on echocardiography or MRI. They underwent CTA for thoracic complaints requiring coronary analysis, which proved negative. All patients provided written informed consent.

Explanted heart experiments

Langendorff-perfused explanted heart experiments were performed on six porcine hearts and one human donor heart. Procurement and use of the human donor heart with informed consent from family members were approved by the French National Biomedical Agency and in a manner conforming to the Declaration of Helsinki. The animal study was carried out in accordance with the recommendations of the Directive 2010/63/EU of the European Parliament on the protection of animals used for scientific purposes and approved by the local ethical committee of Bordeaux CEEA50.

The pig hearts were from males with an average age of 3 months and weight of 38.5 ± 1.8 kg. The human heart was from a 76-year-old female (weight, 50 kg) who died of ischemic stroke and had a history of hypertension; her heart was rejected for human transplantation because of her age. The hearts were explanted and put in a Langendorff setup with retrograde perfusion of the aorta. Repolarization substrate was mimicked by creating local regions of early and late repolarization. This was achieved by providing these Langendorff-perfused hearts with a separate infusion of the LAD coronary artery and the remaining (aorta-perfused) coronary arteries (fig. S2A). Hearts were perfused with a 1:9 mixture of blood and Tyrode's solution, oxygenated with 95%/5% O_2/CO_2 (pH 7.4, 37°C). Dofetilide, blocking the potassium current I_{Kr} in cardiomyocytes, was infused in the aorta, resulting in local RT prolongation at the posterior side of the heart. Pinacidil, activating ATP (adenosine 5′-triphosphate)–sensitive potassium channels, was infused in the LAD, resulting in local RT shorting at the anterior side of the heart. A 108-electrode sock (fig. S2B) wrapped around the heart provided EGM recordings from which local RTs were determined. By placing the heart in a tank shaped like a human torso with 256 electrodes and filled with perfusate, simultaneous body-surface ECGs could be obtained (fig. S2C) (*30*).

A pair of bipolar pacing electrodes on the atria was used to provide a baseline paced rhythm to mimic normally conducted sinus rhythm ("S1 pacing"). To test arrhythmia inducibility, after a train of eight S1 beats, a single ventricular stimulus was provided ("S2 pacing") at one of three available pacing electrodes: the left side of the LAD (LAD-LV), the right side of the LAD (LAD-RV), and the posterior side of the heart (POST). From these pacing locations, the refractory period was defined as the shortest S1-S2 interval where the S2 beat was still conducted (either as a single beat or leading to an arrhythmia). This was usually tested with 10-ms intervals. When capture was detected without arrhythmia, 1-ms intervals were used to determine the refractory period with higher resolution. Arrhythmia inducibility was considered positive when pacing from these electrodes resulted in a sustained arrhythmia (VT or VF) for at least 30 s. If an arrhythmia was induced, the heart was defibrillated after 30 s to restore normal rhythm. During arrhythmia, perfusion to the heart was kept intact and there was no ischemia. In some cases, the protocol had to be aborted early if ischemia was increasing or arrhythmias could not be cardioverted.

A drug infusion protocol was used to create RT differences. Dofetilide target concentration was taken from literature as 100 nM in a no-blood preparation (*31*). To compensate for the use of blood, we corrected for known plasma binding of 60 to 70% of dofetilide (*32*) by multiplying this concentration by 2.5, resulting in a 250 nM target concentration. Pinacidil target concentration from literature was 20 μM in a no-blood preparation (*6*) and multiplied by 1.67 to compensate for its 40% plasma binding (*33*), yielding a final target concentration of 35 μM. Both drugs were also infused at half concentrations (125 nM for dofetilide and 17.5 μM for pinacidil) to test gradual increases. Each drug was infused for at least 15 min before testing arrhythmia inducibility and taking recordings. The drugs were given in the following order (table S1): baseline (no drugs), dofetilide at 125 nM ("Dof 1/2") and 250 nM ("Dof 1/1") in the aorta-perfused region (thus everywhere except LAD), and, on top of Dof 1/1, an additional infusion of pinacidil at 17.5 μM ("Dof 1/1 + Pin 1/2") and 35 μM ("Dof 1/1 + Pin 1/1") in the LAD, followed by washout. This resulted in regions with pronounced RT prolongation (in the non-LAD region) and RT shortening (in the LAD region) with steep gradients at their border.

Use of the "epicardial T wave" upslope as a marker for RT

The T wave on the 12-lead ECG represents the cardiac repolarization phase. In local intracardiac EGMs, the repolarization wave ("intracardiac T wave" or "epicardial T wave") is not completely understood. In particular, the relationship between the morphology of the repolarization wave of local unipolar EGMs and local RT remains a topic of debate and has not been validated in pronounced RT dispersion. In the ex vivo setup described, we studied the time of upslope of the repolarization wave (t_{up}) in epicardial unipolar EGMs as marker of time of local refractoriness (t_{refr}; a surrogate for RT) in intact hearts with RT dispersion. t_{up} was determined from recorded unipolar EGMs. Pacing was used to determine t_{refr}, defined as the shortest coupling interval with capture. Both local metrics were determined relative to global R-peak in the root mean square of the body-surface potentials. In seven hearts (including some that were not included in the main manuscript), selective dofetilide and pinacidil infusion resulted in pronounced regions

with negative and positive repolarization waves, respectively (see fig. S3). Investigating this in more detail, fig. S4 illustrates the correlation between EGM upslope and local refractory time. Thus, the moment of steepest upslope of the repolarization wave in a unipolar epicardial EGM accurately reflects end of local refractoriness in intact hearts, even in pronounced RT dispersion, under these conditions. When local RT is defined by moment of reexcitability (allowing to link it to conduction block and reentry), repolarization wave upslope can be taken as a reliable marker of local RT.

Results from an explanted human heart

In an explanted human heart, the refractory time at that location became much earlier during pinacidil infusion in the LAD (fig. S6). This resulted in a large RTG between the LAD and POST regions. In line with the ex vivo porcine heart results, this resulted in a large vulnerable window for which S1-S2 pacing yielded sustained arrhythmias. During dofetilide infusion in the POST region, the RTG was much smaller. In line with the ex vivo porcine heart results, this resulted in a smaller vulnerable window. After drug washout, the RTG was absent, and no arrhythmias could be induced. In all cases, arrhythmias could only be induced when S2 was from the early RT region, not from the late RT region, confirming the ex vivo porcine heart results.

In silico experiments

Computational ventricular experiments were performed with a previously published human ventricular model (*13*). Two regions were created: a region reflecting the LAD-perfused tissue versus the rest of the heart. In the first region, the conductance of the potassium channel I_{Kr} was increased to shorten the action potential duration (APD), decreasing the local RT; in the latter region, the conductance of I_{Kr} was decreased to prolong the APD, increasing the local RT. We changed the conductance in these regions to create three different in silico heart models, resulting in an APD difference over the transition zone of 74, 126, and 190 ms, respectively. In conjunction with these "small," "medium," and "large" RTGs, we also varied the size of the affected regions from a small, medium, to large LAD-perfused region. Combined, this resulted in nine different heart models with varying areas of abnormalities and varying degrees of gradient steepness. All models were initialized with a baseline "S1" paced rhythm mimicking sinus rhythm. Subsequently, arrhythmia inducibility was tested on selected locations by providing a single ventricular stimulus "S2" at 10-ms increments after the last S1 stimulus.

Electrocardiographic imaging

The patients underwent ECGI as previously described and validated (fig. S10) (*11*, *12*). In brief, 184 Ag-AgCl electrodes (BioSemi) were attached to the torso of the individual to record body-surface potentials at 2-kHz sampling rate for at least 10 min and typically 1 hour. A CT scan of the heart with intravenous contrast was performed, as well as a low-dose thoracic CT scan to image the electrode positions. From these, a 184-electrode torso and ~2000-node cardiac geometry were digitized, enabling the determination of the electrostatic relationship between the torso electrodes and epicardial ventricular nodes. Previously detailed ECGI methods were used to reconstruct epicardial ventricular EGMs for selected beats (*11*). For each EGM, the activation time and recovery time were determined from the steepest downslope (of the activation complex) and steepest upslope (of the repolarization wave), respectively; this was done with a spatiotemporal approach that took into account the EGM morphology of neighboring nodes to reduce the influence of outliers and noise (*11*). EGMs were disregarded at the "artificial" (ECGI-required) base of the ventricles. EGMs with a low repolarization-wave amplitude were manually disregarded as well (on average, 13% of nodes). When PVCs were captured during the ECGI procedure, all PVCs with distinct morphology were analyzed to determine their origin.

Data processing

RTs recorded with experimental sock electrodes (for the explanted hearts) or with ECGI (in the clinical study) were determined from epicardial EGMs after several postprocessing steps. Details can be found in the Supplementary Materials (figs. S17 to S19). RT was defined as the steepest upslope of the local epicardial EGM (which accurately reflected the time of local refractoriness; fig. S4) and filtered with a 15-mm spatial filter. For each epicardial node, its local RTG (in ms/cm) was then defined as the largest local gradient (RT difference divided by internode distance) in a 10-mm region. Subsequently, for each patient, a single value for RTG (in ms/cm) was defined as the maximum over all local RTGs. In addition, to each RT histogram (colored bars in Fig. 5C), a Kernel distribution with a width of 10 ms was fitted (black line in Fig. 5C) to determine the number of peaks in this distribution, reflecting the number of distinct RT zones in each sinus beat. The origins of PVCs were determined from spatially smoothed activation isochrones with ECGI as described previously (*11*). PVCs were considered "clinically suspect" when their 12-lead ECG morphology during the ECGI recording was similar to PVCs that initiated doublets or triplets, nonsustained VT, sustained VT, or VF during clinical follow-up.

Statistical analysis

For the nonnormally distributed clinical data, the Mann-Whitney *U* test was used to assess group differences, with two-tailed tests for all metrics except PVC coupling interval (which, based on previous data, was suspected to be shorter in idiopathic VF survivors). To compare the occurrence of substrate and trigger elements between idiopathic VF individuals versus controls and PVC individuals versus controls, a one-sided Fisher's exact test was used. For the group characteristics in table S2, a Kruskal-Wallis one-way analysis of variance was performed to study differences in baseline characteristic distributions for the numerical variables; a χ^2 test was used for nominal variables (sex). Statistical outcomes were deemed significant when $P < 0.05$.

SUPPLEMENTARY MATERIALS

www.science.org/doi/10.1126/scitranslmed.abi9317
Materials and Methods
Figures S1 to S20
Tables S1 to S3
Data files S1 and S2
References (*34*, *35*)

View/request a protocol for this paper from *Bio-protocol*.

REFERENCES AND NOTES

1. S. G. Priori, C. Blomström-Lundqvist, A. Mazzanti, N. Blom, M. Borggrefe, J. Camm, P. M. Elliott, D. Fitzsimons, R. Hatala, G. Hindricks, P. Kirchhof, K. Kjeldsen, K.-H. Kuck, A. Hernandez-Madrid, N. Nikolaou, T. M. Norekvål, C. Spaulding, D. J. Van Veldhuisen; ESC Scientific Document Group, 2015 ESC Guidelines for the management of patients

with ventricular arrhythmias and the prevention of sudden cardiac death: The Task Force for the management of patients with ventricular arrhythmias and the prevention of sudden cardiac death of the European Society of Cardiology (ESC). Endorsed by: Association for European Paediatric and Congenital Cardiology (AEPC). *Eur. Heart J.* **36**, 2793–2867 (2015).
2. A. B. de Luna, P. Coumel, J. F. Leclercq, Ambulatory sudden cardiac death: Mechanisms of production of fatal arrhythmia on the basis of data from 157 cases. *Am. Heart J.* **117**, 151–159 (1989).
3. S. M. Al-Khatib, W. G. Stevenson, M. J. Ackerman, W. J. Bryant, D. J. Callans, A. B. Curtis, B. J. Deal, T. Dickfeld, M. E. Field, G. C. Fonarow, A. M. Gillis, C. B. Granger, S. C. Hammill, M. A. Hlatky, J. A. Joglar, G. N. Kay, D. D. Matlock, R. J. Myerburg, R. L. Page, 2017 AHA/ACC/HRS guideline for management of patients with ventricular arrhythmias and the prevention of sudden cardiac death. *J. Am. Coll. Cardiol.* **72**, e91–e220 (2018).
4. M. Visser, J. F. van der Heijden, P. A. Doevendans, P. Loh, A. A. Wilde, R. J. Hassink, Idiopathic ventricular fibrillation: The struggle for definition, diagnosis, and follow-up. *Circ. Arrhythm. Electrophysiol.* **9**, e003817 (2016).
5. N. Chiamvimonvat, Y. Chen-Izu, C. E. Clancy, I. Deschenes, D. Dobrev, J. Heijman, L. Izu, Z. Qu, C. M. Ripplinger, J. I. Vandenberg, J. N. Weiss, G. Koren, T. Banyasz, E. Grandi, M. C. Sanguinetti, D. M. Bers, J. M. Nerbonne, Potassium currents in the heart: Functional roles in repolarization, arrhythmia and therapeutics. *J. Physiol.* **595**, 2229–2252 (2017).
6. R. Coronel, F. J. G. Wilms-Schopman, T. Opthof, M. J. Janse, Dispersion of repolarization and arrhythmogenesis. *Heart Rhythm* **6**, 537–543 (2009).
7. R. Vijayakumar, J. N. A. Silva, K. A. Desouza, R. L. Abraham, M. Strom, F. Sacher, G. F. Van Hare, M. Haïssaguerre, D. M. Roden, Y. Rudy, Electrophysiologic substrate in congenital long QT syndrome. *Circulation* **130**, 1936–1943 (2014).
8. J. Zhang, F. Sacher, K. Hoffmayer, T. O'Hara, M. Strom, P. Cuculich, J. Silva, D. Cooper, M. Faddis, M. Hocini, M. Haïssaguerre, M. Scheinman, Y. Rudy, Cardiac electrophysiological substrate underlying the ECG phenotype and electrogram abnormalities in Brugada syndrome patients. *Circulation* **131**, 1950–1959 (2015).
9. J. Zhang, M. Hocini, M. Strom, P. S. Cuculich, D. H. Cooper, F. Sacher, M. Haïssaguerre, Y. Rudy, The electrophysiological substrate of early repolarization syndrome. *JACC Clin. Electrophysiol.* **3**, 894–904 (2017).
10. Y. Wang, P. S. Cuculich, J. Zhang, K. A. Desouza, R. Vijayakumar, J. Chen, M. N. Faddis, B. D. Lindsay, T. W. Smith, Y. Rudy, Noninvasive electroanatomic mapping of human ventricular arrhythmias with electrocardiographic imaging. *Sci. Transl. Med.* **3**, 98ra84 (2011).
11. M. J. M. Cluitmans, P. Bonizzi, J. M. H. Karel, M. Das, B. L. J. H. Kietselaer, M. M. J. de Jong, F. W. Prinzen, R. L. M. Peeters, R. L. Westra, P. G. A. Volders, In vivo validation of electrocardiographic imaging. *JACC Clin. Electrophysiol.* **3**, 232–242 (2017).
12. L. R. Bear, M. Cluitmans, E. Abell, J. Rogier, L. Labrousse, L. K. Cheng, I. LeGrice, N. Lever, G. B. Sands, B. Smaill, M. Haïssaguerre, O. Bernus, R. Coronel, R. Dubois, Electrocardiographic imaging of repolarization abnormalities. *J. Am. Heart Assoc.* **10**, e020153 (2021).
13. J. D. Bayer, G. G. Lalani, E. J. Vigmond, S. M. Narayan, N. A. Trayanova, Mechanisms linking electrical alternans and clinical ventricular arrhythmia in human heart failure. *Heart Rhythm* **13**, 1922–1931 (2016).
14. A. Leenhardt, E. Glaser, M. Burguera, M. Nürnberg, P. Maison-Blanche, P. Coumel, Short-coupled variant of torsade de pointes. A new electrocardiographic entity in the spectrum of idiopathic ventricular tachyarrhythmias. *Circulation* **89**, 206–215 (1994).
15. K. M. W. Leong, F. S. Ng, C. Roney, C. Cantwell, M. J. Shun-Shin, N. W. F. Linton, Z. I. Whinnett, D. C. Lefroy, D. W. Davies, S. E. Harding, P. B. Lim, D. Francis, N. S. Peters, A. M. Varnava, P. Kanagaratnam, Repolarization abnormalities unmasked with exercise in sudden cardiac death survivors with structurally normal hearts. *J. Cardiovasc. Electrophysiol.* **29**, 115–126 (2018).
16. G. Tse, M. Gong, W. T. Wong, S. Georgopoulos, K. P. Letsas, V. S. Vassiliou, Y. S. Chan, B. P. Yan, S. H. Wong, W. K. K. Wu, A. Ciobanu, G. Li, J. Shenthar, A. M. Saguner, S. Ali-Hasan-Al-Saegh, A. Bhardwaj, A. C. Sawant, P. Whittaker, Y. Xia, G.-X. Yan, T. Liu, The T_{peak} - T_{end} interval as an electrocardiographic risk marker of arrhythmic and mortality outcomes: A systematic review and meta-analysis. *Heart Rhythm* **14**, 1131–1137 (2017).
17. B. J. D. Boukens, M. Dacey, V. M. F. Meijborg, M. J. Janse, J. Hadaya, P. Hanna, M. A. Swid, T. Opthof, J. Ardell, K. Shivkumar, R. Coronel, Mechanism of ventricular premature beats elicited by left stellate ganglion stimulation during acute ischemia of the anterior left ventricle. *Cardiovasc. Res.* **31**, 2083–2091 (2020).
18. I. Goldenberg, A. J. Moss, Long QT syndrome. *J. Am. Coll. Cardiol.* **51**, 2291–2300 (2008).
19. M. R. Rivaud, J. D. Bayer, M. Cluitmans, J. van der Waal, L. R. Bear, B. J. Boukens, C. Belterman, L. Gottlieb, F. Vaillant, E. Abell, R. Dubois, V. M. F. Meijborg, R. Coronel, Critical repolarization gradients determine the induction of reentry-based torsades de Pointes arrhythmia in models of long QT syndrome. *Heart Rhythm* **18**, 278–287 (2021).
20. M. Haïssaguerre, J. Duchateau, R. Dubois, M. Hocini, G. Cheniti, F. Sacher, T. Lavergne, V. Probst, E. Surget, E. Vigmond, N. Welte, R. Chauvel, N. Derval, T. Pambrun, P. Jais, W. Nademanee, O. Bernus, Idiopathic ventricular fibrillation. *JACC Clin. Electrophysiol.* **6**, 591–608 (2020).
21. J. A. Chiladakis, G. Karapanos, P. Davlouros, G. Aggelopoulos, D. Alexopoulos, A. S. Manolis, Significance of r-on-t phenomenon in early ventricular tachyarrhythmia susceptibility after acute myocardial infarction in the thrombolytic era. *Am. J. Cardiol.* **85**, 289–293 (2000).
22. F. C. Kempf Jr., M. E. Josephson, Cardiac arrest recorded on ambulatory electrocardiograms. *Am. J. Cardiol.* **53**, 1577–1582 (1984).
23. M. B. Liu, N. Vandersickel, A. V. Panfilov, Z. Qu, R-from-T as a common mechanism of arrhythmia initiation in long QT syndromes. *Circ. Arrhythm. Electrophysiol.* **12**, e007571 (2019).
24. J. M. De Bakker, F. J. Van Capelle, M. J. Janse, A. A. Wilde, R. Coronel, A. E. Becker, K. P. Dingemans, N. M. Van Hemel, R. N. Hauer, Reentry as a cause of ventricular tachycardia in patients with chronic ischemic heart disease: Electrophysiologic and anatomic correlation. *Circulation* **77**, 589–606 (1988).
25. B. J. Boukens, M. Potse, R. Coronel, Fibrosis and conduction abnormalities as basis for overlap of Brugada syndrome and early repolarization syndrome. *Int. J. Mol. Sci.* **22**, 1570 (2021).
26. R. Coronel, M. J. Janse, T. Opthof, A. A. Wilde, P. Taggart, Postrepolarization refractoriness in acute ischemia and after antiarrhythmic drug administration: Action potential duration is not always an index of the refractory period. *Heart Rhythm* **9**, 977–982 (2012).
27. G. O'Grady, T. L. Abell, Gastric arrhythmias in gastroparesis. *Gastroenterol. Clin. North Am.* **44**, 169–184 (2015).
28. W. Wu, H. Wang, P. Zhao, M. Talcott, S. Lai, R. C. McKinstry, P. K. Woodard, G. A. Macones, A. L. Schwartz, A. G. Cahill, P. Cuculich, Y. Wang, Noninvasive high-resolution electromyometrial imaging of uterine contractions in a translational sheep model. *Sci. Transl. Med.* **11**, eaau1428 (2019).
29. G. Cheniti, K. Vlachos, M. Meo, S. Puyo, N. Thompson, A. Denis, J. Duchateau, M. Takigawa, C. Martin, A. Frontera, T. Kitamura, A. Lam, F. Bourier, N. Klotz, N. Derval, F. Sacher, P. Jais, R. Dubois, M. Hocini, M. Haissaguerre, Mapping and ablation of idiopathic ventricular fibrillation. *Front. Cardiovasc. Med.* **5**, 123 (2018).
30. L. R. Bear, R. D. Walton, E. Abell, Y. Coudière, M. Haissaguerre, O. Bernus, R. Dubois, Optical imaging of ventricular action potentials in a torso tank: A new platform for non-invasive electrocardiographic imaging validation. *Front. Physiol.* **10**, 146 (2019).
31. M. Laursen, M. Grunnet, S.-P. Olesen, T. Jespersen, T. Mow, Keeping the rhythm—Pro-arrhythmic investigations in isolated Göttingen minipig hearts. *J. Pharmacol. Toxicol. Methods* **64**, 134–144 (2011).
32. National Center for Biotechnology Information, Dofetilide, CID=71329PubChem Database; https://pubchem.ncbi.nlm.nih.gov/compound/Dofetilide#section=Absorption-Distribution-and-Excretion.
33. J. W. Ward, A. McBurney, P. R. Farrow, P. Sharp, Pharmacokinetics and hypotensive effect in healthy volunteers of pinacidil, a new potent vasodilator. *Eur. J. Clin. Pharmacol.* **26**, 603–608 (1984).
34. K. H. W. J. ten Tusscher, A. V. Panfilov, Alternans and spiral breakup in a human ventricular tissue model. *Am. J. Physiol. Heart Circ. Physiol.* **291**, H1088–H1100 (2006).
35. E. J. Vigmond, R. Weber dos Santos, A. J. Prassl, M. Deo, G. Plank, Solvers for the cardiac bidomain equations. *Prog. Biophys. Mol. Biol.* **96**, 3–18 (2008).

Funding: This work was supported by the Hein Wellens Foundation, Health Foundation Limburg (Maastricht, The Netherlands), and a Veni grant from the Netherlands Organization for Scientific Research (TTW16772) to M.J.M.C.; Kootstra Talent Fellowship research grant from Maastricht University and a research grant from the Dutch Heart Foundation (2015T61) to U.C.N.; and the Netherlands CardioVascular Research Initiative (CVON2017-13 VIGILANCE and CVON2018B030 PREDICT2), Den Haag, The Netherlands to P.G.A.V. This work was furthermore supported by the French National Research Agency (ANR-10-IAHU04-LIRYC) and the Leducq foundation transatlantic network of excellence RHYTHM network (16CVD02). **Author contributions:** Conceptualization: M.J.M.C., L.R.B., R.C., and P.G.A.V. Methodology: M.J.M.C., L.R.B., R.C., P.G.A.V., J.B., C.N.W.B., and E.A. Investigation: M.J.M.C., L.R.B., R.C., J.B., C.N.W.B., E.A., U.C.N., B.v.R., J.S., C.M., and K.D.L. Funding acquisition: M.J.M.C., O.B., M.H., R.J.H., R.D., and P.G.A.V. Writing—original draft: M.J.M.C., L.R.B., R.C., and P.G.A.V. Writing—review and editing: all authors. **Competing interests:** C.M. has received speaker's fees from Bayer Healthcare. The other authors declare that they have no competing interests. **Data and materials availability:** All data associated with this study are present in the paper or the Supplementary Materials.

Submitted 9 April 2021
Accepted 27 October 2021
Published 17 November 2021
10.1126/scitranslmed.abi9317

Science Translational Medicine

Noninvasive detection of spatiotemporal activation-repolarization interactions that prime idiopathic ventricular fibrillation

Matthijs J. M. CluitmansLaura R. BearUyên C. NguyênBianca van ReesJob StoksRachel M. A. ter BekkeCasper MihlJordi HeijmanKevin D. LauEdward VigmondJason BayerCharly N. W. BeltermanEmma AbellLouis LabrousseJulien RogierOlivier BernusMichel HaïssaguerreRutger J. HassinkRémi DuboisRuben CoronelPaul G. A. Volders

Sci. Transl. Med., 13 (620), eabi9317. • DOI: 10.1126/scitranslmed.abi9317

Detecting arrhythmogenic electrical interactions

The interactions between triggers for ventricular fibrillation (VF) and subtle repolarization abnormalities of the heart have been difficult to study because these changes are not typically detected on a standard electrocardiogram. Here, Cluitmans and colleagues combined perfused explanted human and pig heart studies with computational modeling and electrocardiographic imaging of survivors of idiopathic VF to better understand how the steepness of repolarization time (RT) gradients and the sizes of different repolarization regions contributed to idiopathic VF development. The authors found that the timing of a premature beat and its origination from an early RT region, as well as the presence of a steep RT gradient and the sizes of regions with early and late repolarization, led to the development of idiopathic ventricular fibrillation, suggesting that targeted interventions may be possible.